

Walking and conformal dynamics in many-flavor QCD

**Yasumichi Aoki^a, Tatsumi Aoyama^a, Ed Bennett^b, Masafumi Kurachi^c,
Toshihide Maskawa^a, Kohtaroh Miura^d, Kei-ichi Nagai^a, Hiroshi Ohki^{*e},
Enrico Rinaldi^f, Akihiro Shibata^g, Koichi Yamawaki^a, and Takeshi Yamazaki^h**
(LatKMI Collaboration)

^a Kobayashi-Maskawa Institute for the Origin of Particles and the Universe (KMI), Nagoya University, Nagoya, 464-8602, Japan

^b Department of Physics, Swansea University, Singleton Park, Swansea SA2 8PP, UK

^c Institute of Particle and Nuclear studies, High Energy Accelerator Research Organization (KEK), Tsukuba 305-0801, Japan

^d Centre de Physique Théorique (CPT), Aix-Marseille University, Campus de Luminy, Case 907, 163 Avenue de Luminy, 13288 Marseille cedex 9, France

^e RIKEN BNL Research center, Brookhaven National Laboratory, Upton, NY, 11973, USA

^f Lawrence Livermore National Laboratory, Livermore, California, 94550, USA

^g Computing Research Center, High Energy Accelerator Research Organization (KEK), Tsukuba 305-0801, Japan

^h Graduate School of Pure and Applied Sciences, University of Tsukuba, Tsukuba, Ibaraki 305-8571, Japan

In the search for a realistic walking technicolor model, QCD with many flavors is an attractive candidate. From the series of studies by the LatKMI collaboration, we present updated results of the scaling properties of various hadron spectra, including the (pseudo)scalar, vector, and baryon channels, for $N_f = 8$ QCD analyzed with the HISQ action. By comparing these with $N_f = 12$ QCD, which has properties consistent with conformality, possible signals of walking dynamics are discussed. We also present a preliminary result of the flavor-singlet pseudoscalar mass in many-flavor QCD.

*The 33rd International Symposium on Lattice Field Theory
14 -18 July 2015
Kobe International Conference Center, Kobe, Japan**

*Speaker.

1. Introduction

SU(3) gauge theory with many flavors is a very good candidate for a walking technicolor model. The LatKMI collaboration has been systematically investigating the SU(3) gauge theory with N_f fundamental fermions with $N_f = (0, 4, 8, 12, \text{ and } 16)$ using a common setup of the lattice action. We utilize the Highly improved staggered quark (HISQ) action with tree-level Symanzik gauge action (HISQ/tree). Our previous results suggested that $N_f = 8$ QCD could have a walking behavior [1]. Similar results were also given in [2]. More interestingly, the flavor-singlet scalar mass is found to be as light as the Nambu-Goldstone (NG) pion (π) in $N_f = 8$ QCD [3]. In this proceeding, we present our updated results of the scaling properties of various hadron spectra, including the pseudoscalar mass (M_π), decay constant (F_π), vector mass (M_ρ), and nucleon mass (M_N) in comparison with $N_f = 12$ QCD. We also present a new result of the measurement of the flavor-singlet pseudoscalar (η') mass for the first time in the many flavor QCD. The mass of η' meson is interesting, since the fermion loop contribution, which would naturally enhance as N_f increases, plays an essential role. Using a topological charge density operator and the gradient flow we can obtain a good signal for the η' meson two-point function. All the updated results shown here are preliminary.

2. Simulation setup and simple analysis

We have been generating configurations at $\beta = 3.8$ with lattice volumes $(L, T) = (18, 24), (24, 32), (30, 40), (36, 48)$ and $(42, 56)$, for various fermion masses. Compared to our previous results in Ref. [1], we have added new simulation points in the smaller mass region of $m_f = 0.012$ and 0.015 on $L = 42$ with 2, 200 and 4, 760 HMC trajectories, and accumulated more configurations at smaller masses on larger volumes. We have now typically ten times many trajectories than the previous data for smaller mass region. The details of simulation parameters and updated results can be found in Ref. [4], where we should mention that some spectrum data have been changed at the 1σ level from the previous results. This is due to the fact that there are unexpectedly long auto correlation lengths for HMC history, which appeared also in the topological history presented in Ref. [5]. In the present analysis, taking a longer HMC trajectory with smaller fermion masses, we obtain more reliable results, which enable us to deeply investigate the scaling behavior of the various hadron spectra. As shown later, this improvement has affected the numerical result for the finite-size hyperscaling analysis, while the statement that there exists an (approximate) conformal behavior is unchanged.

As a simple analysis, we study dimension-less ratios of the physical quantities as M_ρ/M_π , F_π/M_π , and M_N/M_π as a function of M_π shown in Fig. 1. Those ratios are increasing towards the chiral limit. A similar tendency can be seen in our $N_f = 4$ data, and is clearly different from the one in $N_f = 12$, where we find those ratios have mild M_π dependence, and become a constant in the small- M_π region. As for the ratio analysis, our updated result is consistent with the previous result.

3. Hyperscaling analysis

Although the ratio analysis shows a consistent behavior with the theory having broken chiral symmetry, we can still expect some remnant of the conformal symmetry, if the theory is near the

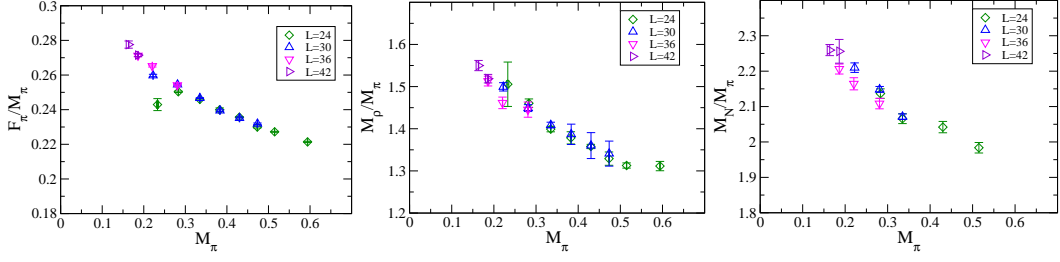


Figure 1: F_π/M_π v.s. M_π (Left), M_ρ/M_π v.s. M_π (Center), and M_N/M_π v.s. M_π (Right) for $N_f = 8$.

edge of the conformal window. In fact, in our previous data we have found that each quantity has an approximate hyperscaling in the intermediate mass region. As shown below, using the updated result with smaller fermion masses, it turns out that this scaling can be seen even at smaller fermion masses. This is one major change in our updated result.

We carry out an individual finite-size hyperscaling fit using a naive function,

$$\xi_h = c_0 + c_1 x, \quad (3.1)$$

where $\xi_h = LM_h$, $h = \pi, \rho$, and N , or $\xi_F = LF_\pi$, and $x = Lm_f^{1/(1+\gamma)}$. In the finite-size hyperscaling analysis we only use the updated data that covers a simulation parameter region with $0.012 \leq m_f \leq 0.08$ and $24 \leq L \leq 42$ ¹. The fit results are shown in Fig. 2 and Table 1. Unlike the previous result (c.f. Table V in Ref. [1]), the naive fit works even in a region of smaller masses except for M_π . The resulting value of γ is $\mathcal{O}(1)$, but it is not universal.

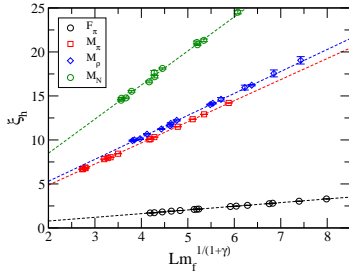


Figure 2: Individual finite-size hyperscaling fit for each ξ_h .

	γ	χ^2/dof
F_π	1.010(6)	1.7
M_π	0.631(3)	19.2
M_ρ	0.904(18)	1.7
M_N	0.838(20)	3.0

Table 1: Result of the naive finite-size hyperscaling fits.

From the mass-deformed conformal theory point of view, non-universality and a large χ^2/dof might be caused by corrections to hyperscaling. To test such a possibility, we carry out a finite-size hyperscaling with mass corrections. Among various types of the mass corrections, we adopt a renormalization group inspired correction term [6] as a benchmark test, which is

$$\frac{\xi_h}{1 + c_2 m^\omega} = c_0 + c_1 x. \quad (3.2)$$

In this formula, there is another exponent ω in the correction term, whose theoretical origin comes down to the critical exponent of the irrelevant operator g (gauge coupling) in the vicinity of the infrared fixed point. As ω can not be analytically determined in the present analysis, we treat it as a fit parameter. Then we carry out the simultaneous finite-size hyperscaling fit for the quantities

¹A full analysis including the previous data with heavier mass region will be presented in Ref. [4].

of F_π , M_π , M_ρ , and M_N with common values of γ and ω . As a comparison we also perform a simultaneous fit without a correction (Eq. 3.1). Both results are shown in Fig. 3, where the vertical axis y in the x - y plane means,

$$y = \begin{cases} \frac{(\xi_h - c_0)/c_1}{x} & \text{(naive fit),} \\ \frac{(\xi_h/(1+c_2 m^\omega) - c_0)/c_1}{x} & \text{(with correction).} \end{cases} \quad (3.3)$$

The data are distributed around the fit line, *i.e.* $y = 1$, where the fitted data with mass correction are closer to the fit line than the naive one. The fit results are tabulated in Table 2. As a result, the mass correction term improves the fit accuracy and we obtain a reasonable χ^2/dof and $\gamma \sim 1$.

However, we should note that in this approach there is no systematic way to incorporate finite mass and volume corrections to the universal hyperscaling relation, and the value of γ depends on the model in general. In addition, the contribution of the correction term for M_π is found to be comparable to that of the naive hyperscaling term in the simulation mass region. Note that c_2 differs depending on the quantity. In this situation, it is not immediately obvious whether each data actually shows a universal scaling towards the chiral limit. (As shown later, there is a clear difference in the correction between $N_f = 8$ and 12.) Even if this is the case, $\gamma(M_\pi) \sim 1$ is also consistent with the chiral broken phase, since it coincides with the leading order of m_f dependence of M_π in the chiral perturbation theory (ChPT) formula². In either case whether $N_f = 8$ QCD is in the conformal phase with $\gamma \sim 1$ or in the chirally broken phase, we can expect that M_π behaves like $M_\pi \sim m_f^{1/2}$ as approaching the chiral limit.

In the next section, in order to see such a scaling behavior, we study mass (scale) dependence of γ for each quantity in detail.

	γ	ω	χ^2/dof
naive fit	0.708(3)	—	84.2
with correction	1.02(4)	0.35(2)	2.3

Table 2: Fit result for simultaneous finite-size hyperscaling with and without a mass correction term.

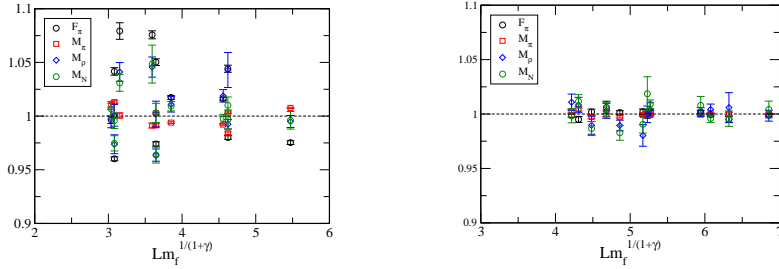


Figure 3: Simultaneous finite-size hyperscaling fit for the naive function (Left), and with correction (Right).

4. Prospect towards the chiral limit

To see a scaling property in detail, we need to systematically study the fermion mass dependence of γ . We consider a window for the fermion mass parameter which corresponds to a range

²In fact, a ChPT-like fit also works in our data, where we can obtain a tiny non-zero F_π in the chiral limit, and the higher order term for M_π^2 is required to fit the data [4].

for three sequential fermion masses, and slide it from $[m_f^{\min}, m_f^{\max}] = [0.012, 0.02]$ to $[0.07, 0.1]$. We then perform a fit for each window. The data on the largest volume are used for each mass, so that we use the naive hyperscaling function $M_h \propto m_f^{1/(1+\gamma)}$. An effective mass anomalous dimension (denoted $\gamma_{\text{eff}}(m_f)$) is calculated as a fit result for each window.

The result for $\gamma_{\text{eff}}(m_f)$ is plotted in the left panel of Fig. 4, where the x -axis means the central value of the fit range. We find that the value of γ_{eff} for M_π increases and it looks like approaching ~ 1 . While our data are far away from the chiral limit, this tendency could be a promising signal for the chirally broken phase. In fact, this result is in sharp contrast to the $N_f = 12$ result, which is shown in the right panel of Fig. 4. In $N_f = 12$, γ_{eff} for M_π never increases towards the chiral limit. Furthermore, γ_{eff} from various quantities tend to become universal in a range of small mass within our statistical accuracy, indicating that the system is in the scaling region. This is consistent with the conformal nature for $N_f = 12$ QCD. A large correction to M_π for $N_f = 8$ found in the previous section could be understood since it is not in the scaling region, while the correction for $N_f = 12$ would become important only when the data outside of the scaling region were included. Although it is obvious within the current data we can not discriminate both possibilities between the strongly coupled conformal theory ($\gamma \sim 1$) and the chiral broken theory with approximate hyperscaling, the tendency of γ_{eff} found in $N_f = 8$ is indicative of a walking gauge theory.

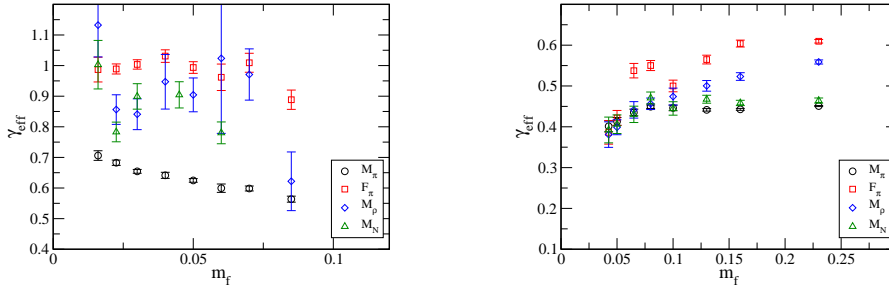


Figure 4: $\gamma_{\text{eff}}(m_f)$ for $N_f = 8$ (Left), and for $N_f = 12$ (Right).

4.1 Effective γ from Dirac eigenvalues

Another way to calculate an effective γ is to use the spectrum of the Dirac eigenvalues. From the density of eigenvalues, $\rho(\lambda)$, with Dirac eigenvalue λ , the scaling law of $\rho(\lambda)$ is given as $\rho(\lambda) \propto \lambda^{\frac{3-\gamma}{1+\gamma}}$. Thus we can obtain a scale-dependent mass anomalous dimension [7]. We define an effective anomalous dimension from Dirac eigenvalues as

$$\frac{3 - \gamma_{\text{eff}}(\lambda)}{1 + \gamma_{\text{eff}}(\lambda)} = \frac{\ln \rho(\lambda + \Delta) - \ln \rho(\lambda)}{\ln(\lambda + \Delta) - \ln \lambda}. \quad (4.1)$$

We show the result for the smallest two fermion masses with $\Delta = 0.004$ in Fig. 5. We find $\gamma_{\text{eff}}(\lambda \sim 0) \sim 3$, which is consistent with a non-zero chiral condensate suffering from a non-zero fermion mass effect. Looking at small λ ($> m_f$), we estimate $0.5 < \gamma_{\text{eff}}(\lambda) \leq 1$ for $0.03 \leq \lambda \leq 0.1$. This is roughly consistent with the one obtained from hadron spectra, but it requires a more careful study.

5. Flavor-singlet pseudoscalar mass

Here we would like to investigate the flavor-singlet pseudoscalar (η'). The η' meson would be a NG-boson of the axial $U(1)$ symmetry of QCD, while its mass is larger compared to the flavor

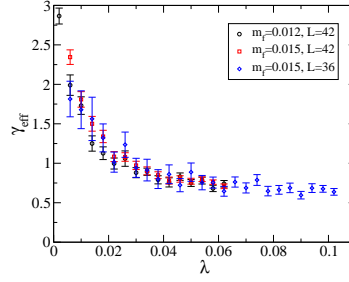


Figure 5: $\gamma_{\text{eff}}(\lambda)$ from Dirac eigenvalue spectrum for $N_f = 8$.

non-singlet pseudoscalar (π), which can be attributed to the axial $U(1)$ anomaly, where the N_f factor manifests in the anomaly contribution. The axial anomaly relation tells that the topology of QCD can also play an important role in the η' meson mass, so that an investigation of the N_f dependence of the mass is important to understand QCD. We use a topological charge density operator $q(x)$ to calculate the two-point correlation function of the η' meson. We use the gradient flow method [8] to improve the statistical accuracy, which was already adopted in the measurement of the topological charge and susceptibility [5]. We measure the correlation function $\langle q(x)q(y) \rangle$ for various flow time t . As a preliminary study we calculate the correlation function at $m_f = 0.02$ on $L = 36$ in $N_f = 8$ ³. The result for the correlation function is shown in the left panel of Fig. 6, where $r = |x - y|$. The mass of the η' meson ($M_{\eta'}$) is obtained by a fit with $\langle q(x)q(y) \rangle = cK_1(M_{\eta'}r)/r$, where $K_1(x)$ is a modified Bessel function and c is a constant. We estimate an effective mass from a fit with range $[r, r + 0.5]$ using an asymptotic form of the above function. The result of the effective mass is shown in the middle panel of Fig. 6. We find that a better plateau is obtained for larger flow time. To see flow time dependence of the mass, we carry out the fit with fixed fit range of $r = 6.5 - 10$. The result is shown in the right panel of Fig. 6, where we find a stable region for $t \leq 1$, and in this region a signal becomes better as t increases. We quote a mass as $M_{\eta'} = 1.00(6)$ at $t = 0.6$ for $m_f = 0.02$. We obtain a ratio $M_{\eta'}/M_\rho = 3.1(2)$. This result is much larger than the real-life QCD. Our result suggests a heavy η' meson, which might be due to a large fermion loop effect in many-flavor QCD.

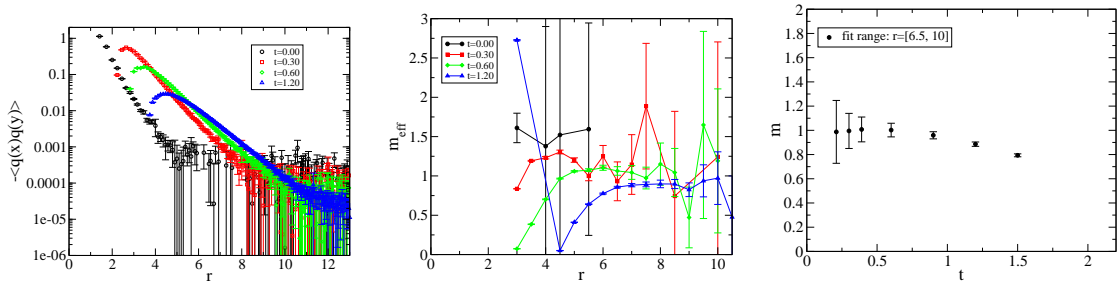


Figure 6: (Left) Two point correlator for η' meson obtained from a topological charge density operator for $N_f = 8$. (Center) The effective mass for the η' meson. (Right) Flow time dependence of the η' meson mass.

³Similar analyses have been done in quenched QCD [9] and 2 + 1 flavor QCD [10].

6. Summary

We have studied the scaling properties of various hadron spectra in $N_f = 8$ QCD. We found that the ratios of the hadron spectra show a similar behavior to the $N_f = 4$ QCD, however, each quantity shows hyperscaling except for M_π , where M_π obviously is outside a scaling region either in the conformal phase or in the chirally broken phase. We also found that a finite-size hyperscaling fit with universal γ can work by adding a mass correction term. The fit result gives $\gamma \sim 1$ and a reasonable χ^2/dof . Further detailed analysis has been performed by studying an effective γ for each hadron spectrum, which turns out to be useful to see a tendency towards the chiral limit. We found a qualitative difference between $N_f = 8$ and 12; in $N_f = 8$ γ_{eff} for M_π is increasing and seems to be approaching ~ 1 towards the chiral limit, while in $N_f = 12$ a universal value of $\gamma_{\text{eff}} \sim 0.4$ can be obtained in a smaller fermion mass region. This result might be indicative of $N_f = 8$ QCD being in the chirally broken phase. As a result, $N_f = 8$ QCD still possesses two possibilities of the strongly coupled conformal theory ($\gamma \sim 1$) and chirally broken theory with walking behavior. Thus $N_f = 8$ QCD is a good candidate for the walking technicolor model. We have also provided a calculation of the flavor-singlet pseudoscalar mass in $N_f = 8$ QCD. Using a gluonic operator and the gradient flow, we have obtained a good signal of the η' mass for the first time in the many flavor QCD. Our result suggests a heavy η' compared to real-life QCD.

Acknowledgments – Numerical computations have been carried out on ϕ at KMI, CX400 at the Information Technology Center in Nagoya University, and CX400 and HA8000 at the Research Institute for Information Technology in Kyushu University. This work is supported by the JSPS Grant-in-Aid for Scientific Research (S) No.22224003, (C) No.23540300 (K.Y.), for Young Scientists (B) No.25800139 (H.O.) and No.25800138 (T.Y.), and also by the MEXT Grants-in-Aid for Scientific Research on Innovative Areas No.23105708 (T.Y.) and No.25105011 (M.K.). This work is supported by the JLDG constructed over the SINET of NII. The work of H.O. is supported by the RIKEN Special Postdoctoral Researcher program. E.R. acknowledges the support of the U.S. Department of Energy under Contract DE-AC52-07NA27344 (LLNL).

References

- [1] Y. Aoki, T. Aoyama, M. Kurachi, T. Maskawa, K.-i. Nagai, H. Ohki, A. Shibata, K. Yamawaki, and T. Yamazaki, (LatKMI Collaboration), Phys. Rev. D **87**, no. 9, 094511 (2013).
- [2] T. Appelquist *et al.* [LSD Collaboration], Phys. Rev. D **90**, no. 11, 114502 (2014).
- [3] Y. Aoki, T. Aoyama, M. Kurachi, T. Maskawa, K. Miura, K. -i. Nagai, H. Ohki, E. Rinaldi, A. Shibata, K. Yamawaki, and T. Yamazaki (LatKMI Collaboration), Phys. Rev. D **89**, 111502 (2014).
- [4] LatKMI Collaboration, in preparation.
- [5] Y. Aoki, T. Aoyama, E. Bennett, M. Kurachi, T. Maskawa, K. Miura, K.-i. Nagai, H. Ohki, E. Rinaldi, A. Shibata, K. Yamawaki, and T. Yamazaki, (LatKMI Collaboration), PoS LATTICE 2015, 214.
- [6] A. Cheng *et al.* Phys. Rev. D **90**, no. 1, 014509 (2014).
- [7] A. Cheng, A. Hasenfratz, G. Petropoulos and D. Schaich, JHEP **1307**, 061 (2013).
- [8] M. Luscher, JHEP **1008**, 071 (2010) [JHEP **1403**, 092 (2014)].
- [9] A. Chowdhury, A. Harindranath and J. Maiti, Phys. Rev. D **91**, no. 7, 074507 (2015).
- [10] H. Fukaya *et al.* [JLQCD Collaboration], arXiv:1509.00944 [hep-lat].